4-15-2005

Ocular surface epithelia contain ABCG2-dependent side population cells exhibiting features associated with stem cells.

Murat T Budak
Department of Ophthalmology, Mount Sinai School of Medicine

Onder S Alpdogan
Department of Medical Oncology, Thomas Jefferson University; Department of Medicine and Pediatrics, Memorial Sloan-Kettering Cancer Center, Seyfettin.Alpdogan@jefferson.edu

Mingyuan Zhou
Department of Dermatology, The Feinberg School of Medicine at Northwestern University

Robert M Lavker
Department of Dermatology, The Feinberg School of Medicine at Northwestern University

M A Murat Akinci
Department of Ophthalmology, Mount Sinai School of Medicine

See next page for additional authors

Let us know how access to this document benefits you

Follow this and additional works at: http://jdc.jefferson.edu/medoncfp

![icon] Part of the Medical Immunology Commons, and the Oncology Commons

Authors

Murat T Budak, Onder S Alpdogan, Mingyuan Zhou, Robert M Lavker, M A Murat Akinci, and J Mario Wolosin

Ocular surface epithelia contain ABCG2-dependent side population cells exhibiting features associated with stem cells

Murat T. Budak[1], Onder S. Alpdogan[2], Mingyuan Zhou[3], Robert M. Lavker[3,*], M.A. Murat Akinci[1] and J. Mario Wolosin[1,*]

[1]Department of Ophthalmology, Mount Sinai School of Medicine, One Gustave L. Levy Place, New York, NY 10029, USA
[2]Department of Medicine and Pediatrics, Memorial Sloan-Kettering Cancer Center, 1275 York Avenue, New York, NY 10021, USA
[3]Department of Dermatology, The Feinberg School of Medicine at Northwestern University, 303 East Chicago Avenue, Chicago, IL 60611, USA
*Authors for correspondence (e-mail: jmario.wolosin@mssm.edu; r-lavker@northwestern.edu)

Summary

When cell populations are incubated with the DNA-binding dye Hoechst 33342 and subjected to flow cytometry analysis for Hoechst 33342 emissions, active efflux of the dye by the ABCG2/BCRP1 transporter causes certain cells to appear as a segregated cohort, known as a side population (SP). Stem cells from several tissues have been shown to possess the SP phenotype. As the lack of specific surface markers has hindered the isolation and subsequent biochemical characterization of epithelial stem cells this study sought to determine the existence of SP cells and expression of ABCG2 in the epithelia of the ocular surface and evaluate whether such SP cells had features associated with epithelial stem cells. Human and rabbit limbal-corneal and conjunctival epithelial cells were incubated with Hoechst 33342, and analyzed and sorted by flow cytometry. Sorted cells were subjected to several tests to determine whether the isolated SP cells displayed features consistent with the stem cell phenotype. Side populations amounting to <1% of total cells, which were sensitive to the ABCG2-inhibitor fumitremorgin C, were found in the conjunctival and limbal epithelia, but were absent from the stem cell-free corneal epithelium. Immunohistochemistry was used to establish the spatial expression pattern of ABCG2. The antigen was detected in clusters of conjunctival and limbal epithelia basal cells but was not present in the corneal epithelium. SP cells were characterized by extremely low light side scattering and contained a high percentage of cells that: showed slow cycling prior to tissue collection; exhibited an initial delay in proliferation after culturing; and displayed clonogenic capacity and resistance to phorbol-induced differentiation; all features that are consistent with a stem cell phenotype.

Key words: Stem cells, Side population, Epithelia, Cornea, Limbus, Conjunctiva

Introduction

The vertebrate ocular surface is lined with two stratified, constantly renewing tissues, the limbal/corneal and conjunctival epithelia. These two closely related but distinct cell lineages (Kruse et al., 1990; Wei et al., 1993; Wei et al., 1996; Moyer et al., 1996), arise simultaneously from a few PAX6-positive ectodermal cells that remain in the embryonic ectodermal surface following formation of the lens vesicle by the bulk of the PAX6+ cells (Davis and Reed, 1996; Koroma et al., 1997; Wolosin et al., 2002).

The self-renewing nature of the limbal/corneal and conjunctival epithelia makes their long-term survival ultimately dependent on small populations of stem cells. In the limbal/corneal epithelia, SCs are exclusively situated in the basal cell layer of the limbus, the outer vascular rim at the junction between the cornea and the conjunctiva (Schemer et al., 1986; Cotsarelis et al., 1989). The epithelium covering the transparent central cornea contains no stem cells (Schermer et al., 1986; Cotsarelis et al., 1989; Wolosin et al., 2000). Several lines of evidence suggest that conjunctival epithelial stem cells are concentrated in the fornix (Wei et al., 1995; Pellegrini et al., 1999), though stem cells may also be present in other areas (Pellegrini et al., 1999; Wirtschafter et al., 1999; Chen et al., 2003; Nagasaki and Zhao, 2005).

The ability to isolate viable somatic stems cells will provide new, invaluable means to characterize these cells and use them in gene therapy protocols (Bradfute and Goodell, 2002). The identification of a number of surface markers has facilitated the routine preparation of hematopoietic stem cells (Civin, 1992; Silvestri, 1992). Identification of comparable markers in epithelial systems has remained a challenging task. An alternative method for the purification of stem cells exploits their special spectral emission pattern following staining with the DNA dye Hoechst 33342 (Hoechst). In the free state the dye exhibits a fluorescence emission peak at 465 nm (Hoechst blue). In the DNA-bound state in live cells, electronic interactions between the densely packed Hoechst molecules cause a bathochromic shift leading to a secondary emission at 675 nm (Hoechst red). Hoechst-stained bone marrow cells subjected to flow cytometry reveal a population of cells displaying very low fluorescent emission intensities and a reduced bathochromic shift. The cohort, or side population

(SP), reflects a reduction of DNA-bound dye in these cells due to their ability to actively efflux Hoechst. The bone marrow SP cells are enriched in hematopoietic cells with multiple stem cell characteristics, including the capacity for long-term lineage reconstitution (Goodell et al., 1996; Uchida et al., 2003).

Recently, it was demonstrated that Hoechst efflux in the SP cells is mediated by the G2 subtype member of the ATP Binding Cassette (ABC) transporter, and the authors proposed that the SP phenotype may be a feature displayed by multiple adult stem cell types (Zhou et al., 2001). Several studies have provided support for this proposal (Scharenberg et al., 2002; Lechner et al., 2002; Kim and Morshead, 2003; Alison, 2003; Lassalle et al., 2003; Bhattacharya et al., 2003; Summer et al., 2003). Preliminary reports on the presence of SP cells in the limbal zone have been published (Watanabe et al., 2004; Wolosin et al., 2004) We describe now the existence of ABCG2-dependent SP cells in the human and rabbit ocular surface epithelia and demonstrate that these cells display many features that are consistent with a stem cell phenotype.

Materials and Methods

Tissue procurement and processing

Rabbit tissues were dissected from eyes obtained from local abattoirs. Human corneas and conjunctivas unsuitable for human transplant, all from unidentifiable donors, were obtained from the National Disease Research Interchange (Philadelphia, PA) within 48 hours of collection. For the cell kinetics studies (see below), 3-month-old albino New Zealand rabbits were housed in an American Association of Laboratory Animal Care-accredited facility with free access to food and water. All animal procedures complied with the USPHS policy on humane care and use of laboratory animals. For limbal dissection, corneas were quartered, and after careful trimming of conjunctival remnants, placed on a black cutting board. Tangential illumination was used to visualize and surgically dissect the rabbit limbus as a discrete 0.5-0.8 mm-wide whitish outer strip and the human limbus as a discrete ~1-mm-wide zone containing the Palisades of Vogt. Tissues were incubated for 16-20 hours at 4°C in 5 mg/ml Dispase (Roche, Indianapolis, IN) dissolved in 4-(2-hydroxyethyl)-1-piperazineethanesulfonic acid-buffered 1:1 mix of Dulbecco's modified Eagle's medium and Ham-F12 (hD/F-12) with moderate shaking. This results in the spontaneous release of whole epithelial sheets.

Flow cytometry

Pure epithelial sheets were incubated for 20-30 minutes at 37°C in trypsin. When >90% of the population consisted of single cells, the suspension was complemented with one volume of hD/F-12 containing 20% fetal calf serum (FCS), cells were dispersed using a fire-polished Pasteur pipette, sequentially filtered through 40 μm and 10 μm nylon meshes, suspended at 10^6 cells/ml in hD/F-12 containing 2% FCS, and incubated with 2-5 μg Hoechst (Sigma, St Louis, MO) for 45-90 minutes at 37°C under slow swirling motion. To inhibit ABC transporters, 10 μM reserpine (Sigma), 10-100 μM verapamil (Sigma) or 10 μM fumitremorgin C (a generous gift from Susan Bates, NCI, Bethesda, MD) were added 5 minutes before the addition of Hoechst. Cells were spun down, resuspended at 10^6 cells/ml in HBSS with 4% FCS and 2 μg/ml propidium iodide (PI; Roche, Indiana, IN), analyzed for fluorescent emissions and side and forward light scattering (SSC and FSC, respectively) and sorted in a MoFlo (Cytomation, Fort Collins, CO) cytometer. Instrument gains were adjusted to set the main cell cohort, which comprises most of the cells containing one copy of DNA (G0 and G1, or G0-G1, cells; see Fig. 1), at the center of the plots. Data for viable cells (PI staining intensity below 1% of the maximal staining) were analyzed for parametric correlations and annotated using FCSExpress (DeNovo Software, Toronto, Canada).

For direct microscopic observation, human limbal cells were spun down and gently resuspended in a minimal volume of HBSS with 0.1% Trypan Blue and examined in an inverted microscope using phase-contrast and transmitted light illuminations.

BrdU labeling in vivo

Three 2ML2 osmotic Alzet mini pumps (Durect, Cupertino, CA) calibrated to produce a constant delivery of ~24 mg bromo-deoxyuridine (BrdU)/day for 14-16 days, were implanted subcutaneously into 3 kg (3-4 months old) rabbits. Most animals were sacrificed 11 days later, when continuous steady state label pumping had proceeded for 10 days. In one case the pumps were removed after 17 days, and the animal was left undisturbed for 38 days prior to sacrifice and tissue collection. Small segments of the limbal/corneal and conjunctival tissues were fixed overnight at 4°C in 50 mM glycine, 70% ethanol, pH 3.0 and embedded in paraffin. The majority of the tissue was used to isolate the limbal and conjunctival epithelium, sort single cell suspensions by flow cytometry and to determine the BrdU content of the sorted fractions.

BrdU detection in tissue sections

Paraffin-embedded tissues were cut into 4-μm-thick sections, deparaffinized, rehydrated in PBS, immersed in 2N HCl for 30 minutes and digested with trypsin for 15 minutes. BrdU incorporation was revealed by indirect immunofluorescence. Sections were blocked in 5% goat serum in PBS and incubated for 2 hours at 37°C with 10 μg/ml anti-BrdU mouse monoclonal antibody (Roche) made in 0.5% Tween 20, 1% goat serum in PBS (T-PBS). After washings, sections were stained for 1 hour with 1 μg/ml Alexa 488-conjugated goat anti-mouse IgG (Molecular Probes, Eugene, OR), counterstained with 0.01% PI-PBS, mounted with anti-fading medium and photographed in an Olympus epifluorescence microscope equipped for green (for Alexa 488), red (for PI) and dual fluorescence image capture.

BrdU detection in sorted cells

Limbal and conjunctival epithelial cells were alternatively sorted according to their Hoechst 33342 staining, or light-scattering properties. Sorted cells were either cytospun onto poly-L-lysine-coated glass slides using a Shandon Cytospin3 centrifuge (Shandon, Wyman, MA) or concentrated and plated overnight on the slides for selection of adherent (i.e. basal) cells. Slides were immersed in 70% ethanol for 30 minutes, briefly air-dried, immersed in 0.07 N NaOH for 2 minutes, overlaid with FITC-conjugated monoclonal anti-BrdU antibody (Pharmingen, San Diego, CA) prepared in T-PBS for 30 minutes, counterstained with 0.01% PI-PBS and mounted and photographed as described above. BrdU-free cells were processed in parallel to serve as controls.

ABCG2 detection in tissue sections

Freshly dissected tissue segments were embedded in Cryomatrix™ (Shandon, Pittsburgh, PA), frozen in liquid nitrogen, cut into 8- to 10-μm-thick sections in a cryotome, collected on gelatin-coated glass slides. The sections were fixed in cold methanol, briefly air-dried, rehydrated in PBS and blocked with 5% goat serum. ABCG2 was detected by indirect immunofluorescence using one of two anti-ABCG2 monoclonal antibodies, BXP21 (Chemicon, Temecula, CA) and BXP34 (Alexis, San Diego, CA) as the primary reagent and Alexa 488 goat anti-mouse IgG as the secondary antibody. Both primary antibodies recognize internal epitopes within the C-terminus of human ABCG2 (Maliepaard et al., 2001). Stained samples were mounted and photographed as described above.

Measurements of initial proliferative rates

Limbal and conjunctival cells (10^6 cells/ml) were incubated for 30 minutes with 0.5 µM carboxy-fluorescein diacetate, succinymidyl ester (CFDA-SE; Molecular Probes). This fluorescein derivative reacts covalently with amino groups resulting in its long-term retention within cells. Thus, decreases in cellular fluorescence reflect primarily cell division (Oostendorp et al., 2000). 100,000 CFDA-SE-loaded epithelial cells were plated on 2.5 cm permeable Falcon tissue culture inserts in which 3T3 cells were plated at 4000 cells/cm^2 on the underside of the permeable synthetic membrane. In one experiment cells were harvested after either 16 or 64 hours, incubated with Hoechst and analyzed in the MoFlo cytometer. In a second experiment, cells were collected after 24 to 96 hours, lightly fixed with 0.1% formaldehyde for 30 minutes and stored at 4°C in 1% BSA. When the last batch of cells was collected, all batches were analyzed by flow cytometry using a FACSCalibur™ Excalibur (BDBiosciences, San Jose, CA) analytical cytometer.

Clonogenic capacity assay

SP and G0-G1 cells were plated at low density (10-50 cells/cm^2) in 20% FCS-hD/F12 onto 100 mm Petri dishes containing a layer of Swiss 3T3 fibroblasts which were incubated with 8 µg/ml mitomycin C (Sigma) for 3 hours to elicit permanent cell proliferation arrest, and then plated at a rate of 2000/cm^2 48 hours prior to epithelial cell addition. Where indicated, phorbol myristate acetate (PMA; Sigma) was added 4 hours later and removed with the first medium refreshment at 72 hours post-plating. For colony visualization, dishes were fixed in cold methanol and incubated for 10 minutes in 50% methanol, 10% acetic acid, 0.01% Coomassie Brilliant Blue R250.

RNA preparation and real-time quantitative PCR

One µg RNA aliquots, isolated using Tri-Reagent (MRC, Cincinnati, HO) and incorporating material from four distinct specimens, were converted into cDNA using reverse transcriptase (Omniscript™; Qiagen, Valencia, CA). No attempt was made to remove residual genomic DNA. An identical mock reaction omitting the enzyme was carried out in parallel. The products of these reactions were subjected to quantitative real-time PCR in an AbiPrism 7900H sequence detection instrument (annealing: 20 seconds at 58°C; DNA melting: 10 seconds at 95°C) using triplicates samples containing QuantiTect™ SYBR® Green PCR mix (Qiagen), reverse-transcribed product derived from 100 ng of initial RNA and primer pairs (150 µM) designed to amplify either ABCG2 (ABCG2fwd: TGCAAC-ATGTACTGGCGAAGA; ABCG2rev: TCTTCCACAAGCCCCA-GG), or β-actin (β-actinfwd: AGTACTCCGTGTGGATCGGC; β-actinrev: GCTGATCCACATCTGCTGGA) (Abbott et al., 2002). The generation of single amplified DNA sequences with the expected size (74 bp for ABCG2 and 68 bp for β-actin), was determined by electrophoresis of the reaction products in 4% agarose gels containing 0.05% Ethidium Bromide. Cycle thresholds (C_t) for the different samples were used to determine relative amounts of ABCG2 message according to the delta-delta C_t method.

Results

Limbal and conjunctival epithelia contain ABCG2-dependent side populations

Initial studies with rabbit cells established the best conditions for the generation of distinguishable SP cells. From these studies we concluded that the optimal Hoechst concentration for the conjunctival epithelium, when performing 90-minute incubations, occurs at 3.0-3.5 µM. For the limbal epithelium better results were obtained by reducing the dye concentration to 2.0-2.5 µM and the incubation time to 60 minutes.

SP cells were present in rabbit and human limbal and conjunctival epithelia (Fig. 1A-D and Table 1). Inclusion of the ABCG2-specific inhibitor fumitremorgin C (Rabindran et al., 2000; Robey et al., 2001; Nakanishi et al., 2003) resulted in a 80-90% reduction in the size of the SPs in both ocular surface epithelia (Fig. 1E,F), confirming that the SP phenotype primarily reflects the activity of the ABCG2 transporter (Zhou et al., 2001). Reserpine, a powerful pan-ABC transporter inhibitor (Zhou et al., 2001; Murayama et al., 2002), completely abolished SP cells (Fig. 1D,F inserts). In contrast, verapamil caused only a 20-30% decrease in rabbit conjunctival SP cells, consistent with the demonstrated lack of effectiveness of this P-glycoprotein inhibitor on ABCG2 activity (Zhou et al., 2001; Ozvegy et al., 2001).

ABCG2 is expressed in the ocular surface epithelia in discreet clusters

The expression of the fumitremorgin C-sensitive ABCG2 transporter was investigated at the mRNA and protein levels.
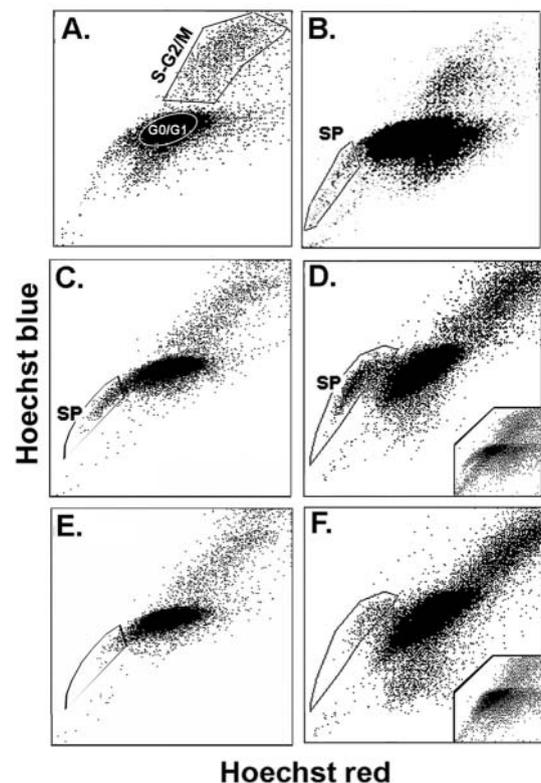

Fig. 1. Hoechst plots of human and rabbit ocular surface epithelial cells. Human (A,B) and rabbit (C-F) limbal cell plots obtained using 2.0 µM dye (left-hand graphs) and conjunctival cell plots using 3.0 µM dye (right-hand graphs). (C,D) Controls. (E,F) Identical experiments to C and D, respectively, but with 10 µM fumitremorgin C added 5 minutes prior to the introduction of Hoechst. Inserts in D and F are a different experiment with rabbit conjunctiva in control condition or with 20 µM reserpine. The three main zones present in these plots, the SP, the main cohort of cells containing one copy of DNA (cells in G0-G1) and the cohort of most cells containing DNA in excess of one copy by virtue of being in the S, G2 or M phase of the cell cycle (S-G2/M) are indicated.

Table 1. SP cell yields for human and rabbit limbal and conjunctival tissues

	N	Total cells/tissue	SP (% viable cells)	SP (% of total)	SP/tissue
Human limbus	6	$5,5 \times 10^5$	0.64	0.49	2695
Human conjunctiva	4	48×10^5	0.92	0.58	27,840
Rabbit limbus	8	$3,3 \times 10^5$	1.21	0.88	2904
Rabbit conjunctiva	16	38×10^5	1.43	0.96	36,840

Percentiles and total cell yields were calculated for each experiment and used to obtain the mean values shown in the table. *N* is the number of replicate experiments.

Real-time quantitative PCR combined with product size confirmation by agarose chromatography (a single 71 bp band; not shown) demonstrated the expression of the message for this protein throughout the ocular surface. Overall message levels were extremely low: in the limbal epithelium ABCG2 they amounted to 1/4800 of the β-actin value. Our measurements indicated very similar message content for the conjunctival and limbal epithelia (ratio=0.96). In contrast, in the stem and SP cell-free corneal epithelium the message amounted to only 1/26.3 of the level measured in the limbal counterpart.

Immunofluorescence detected ABGC2 protein in the periphery of both limbal and conjunctival epithelia cells. Both monoclonal antibodies used generated similar patterns but only results for the clone displaying lower background, BXP21, are shown (Fig. 2). In the limbal/corneal epithelium, ABCG2 antigenicity was observed exclusively in the limbal zone. The stain occurred in cell clusters comprising basal and proximal suprabasal cells. Stain intensity was higher in the cells at the center of each cluster (Fig. 2A-C). The greatest accumulation of such clusters occurred within the Palisades of Vogt (Townsend, 1991), the area generally believed to contain the highest concentration of stem cells within the human limbus. In some of the palisades proximal to the conjunctiva, all basal and suprabasal epithelial cells appeared to be ABCG2-positive. There was no ABCG2 stain in the corneal zone, i.e., the small amount of ABCG2 message expressed in this area did not translate into any visible protein expression (Fig. 2D). In the conjunctival epithelium, ABCG2 stain was detected at low levels in a large fraction of the basal cells throughout the tissue, though it appears to be more intense in the Goblet cell-rich areas (Fig. 2E-G).

Ocular epithelial SP cells display physical and proliferative features consistent with a stem cell phenotype

Analysis of the correlation between light scattering and Hoechst emission features yielded significant insight into physical features of the ocular surface epithelia SP cells (Fig. 3). FSC is generated by particles that are relatively large with respect to the wavelength of the incident light, and thus, this parameter is considered to be proportional to the size of the cell. SSC is generated by particles in the range of, or smaller than, the length of the analyzing beam. Therefore, the magnitude of this signal reflects cell cytosolic and/or cell membrane complexity. The SP cells displayed low FSC, but more significantly, extremely low SSC (LSSC; Fig. 3A). Furthermore, analysis of the correlations between light scattering/Hoechst emission patterns in the opposite direction (Fig. 3B) revealed that only a fraction (~50% in most experiments) of the LSSC cells belong to the SP. To further characterize the SP cells, we compared these cells with cells collected from the core of the main cell cohort (G0-G1, see Fig. 1). Whereas G0-G1 cells ranged in size from between 12-

Fig. 2. ABCG2 immunolocalization in the ocular surface. A. Whole human limbus. To generate this micrograph, multiple frames were spliced together. Note that ABCG2 is intensively expressed in the recedes of the Palisades of Vogt (Pal. Vogt), in particular near the conjunctiva. The immunostaining pattern suggests a cluster organization. Individual clusters are marked by asterisks. (B) High magnification micrograph of a single Palisade of Vogt. (C) The section adjacent to that stained in B was processed with the omission of the anti-ABCG2 antibody

as a control. (D) Human corneal central epithelium. BL, Bowman layer. (E-G) Selected images of the human conjunctiva. ABCG2 expression is extremely low in the very thick palpebral zone (E). It is moderately present in the thinner transition area (F) and at higher levels in the Goblet cell-rich palpebral-fornical zone (G). Asterisks indicate Goblet cells. Magnifications: A,G 120×; B,C,E,F 250×; D 400×.
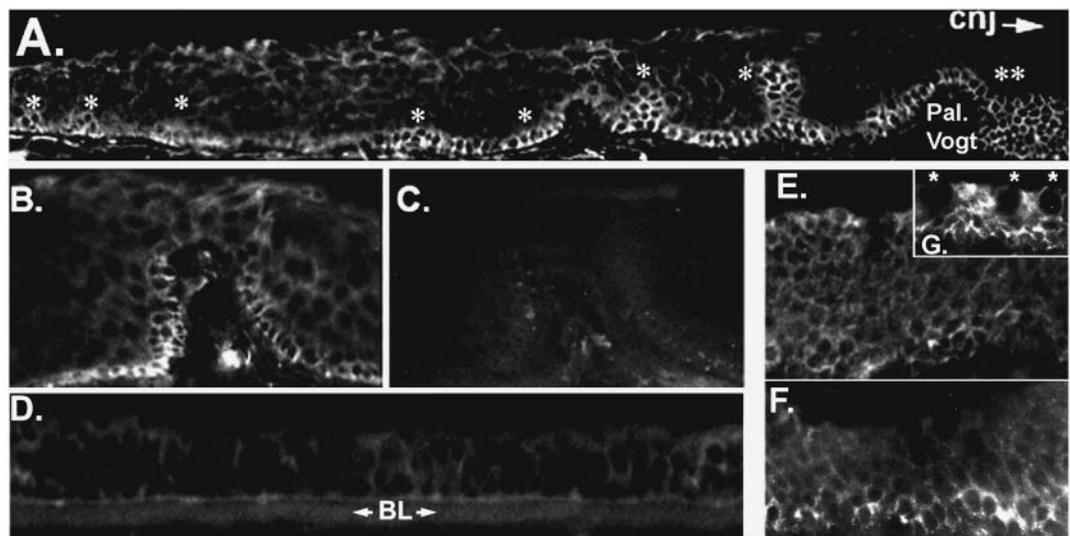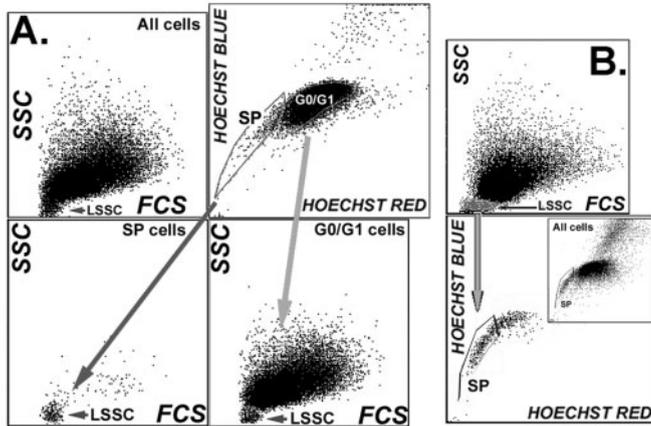
Fig. 3. Reciprocal correlations between Hoechst emission and light scattering features in ocular surface cells. (A) Human limbal epithelium. The scatter plot for all the cells (All cells) shows a main cohort and a small group of cells (LSSC) displaying very low SSC values. Note that ~50% of the SP cells are LCCS cells and that some of the LSSC cells are not SP cells. (B) Representative experiment of the distribution of LSSC cells within the Hoechst plot in the rabbit conjunctiva. Note that the LSSC cells (zone highlighted with a gray mask) distribute equally between the SP and G0-G1 zone. Axis denominations are provided in capital italics within the frames.
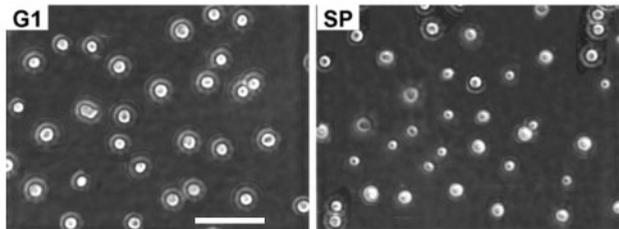

Fig. 4. Phase-contrast micrographs of human limbal epithelial G0-G1 and SP cells. The non-SP cells were collected from the center of the G0-G1 spot. Bar, 30 µm.

18 µm, the SP contained a high proportion of cells with diameters smaller than 10 µm. These cells displayed remarkably low contrast levels (Fig. 4). In addition, examination under regular incident light showed that >95% of the G0-G1 and SP cells excluded Trypan Blue, indicating that the sorting process did not cause any overt cellular damage. Finally, when rabbit or human corneal epithelial cells were subjected to similar analyses, neither SP nor LSSC were detected (Fig. 5).

Several experiments were performed to examine the presumptive stem cell status of the SP cells. Slow or infrequent cycling, is one of the most unique features of adult stem cells (Leblond, 1964; Bickenbach, 1981; Cotsarelis et al., 1989; Pavlovitch et al., 1991; Morris and Potten, 1994; Wei et al., 1995; Fortunel et al., 1998; Lehrer et al., 1998; Braun et al., 2003; Tumbar et al., 2004). Accordingly, we performed experiments aimed at identifying slow- and fast-cycling cells in the conjunctival and limbal epithelia and in their respective flow cytometry cohorts. After 10 days of continuous BrdU infusion, histology revealed that a great proportion of the basal conjunctival (Fig. 6A) and limbal/corneal (Fig. 6D) epithelial cells incorporated BrdU. A substantial fraction of the
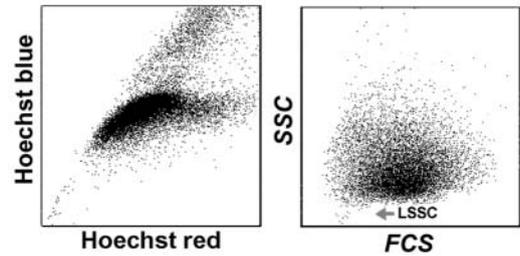

Fig. 5. Hoechst and scatter plots of human corneal cells. Note the complete absence of SP and the paucity of LSSC cells.

suprabasal cells were also stained, reflecting the continuous stratifying activity of these tissues. BrdU$^+$ cells were identified within the sorted populations (Fig. 7E-H). Percentiles of BrdU$^+$ derived from these images are gathered in Table 2. In one experiment (Table 2, experiment number 1) using four rabbits simultaneously, half of the cells for each epithelium were sorted according to Hoechst staining to collect SP and non-SP (taken from the center of G0-G1 cohorts) cells. The other half was sorted according to light scattering properties, to collect LSSC and non-LSSC cells (taken from the center of the main cell group; see Fig. 3). The non-SP, non-LSSC samples, representing the majority of the cells in the population, contained BrdU cells in proportions similar to those observed in the tissue sections. The SP and LSSC fractions displayed much lower percentiles of BrdU$^+$ cells (Fig. 7A,B). In another experiment SP and non-SP (G0-G1) cells were collected from the epithelia of a single rabbit and plated overnight to isolate spontaneously adherent (i.e. basal) cells. For the conjunctiva, 87% of the adherent G0-G1 cells were BrdU$^+$ (Fig. 7C; Table 2, experiment number 2). In contrast, only 9% of the adherent SP cells contained BrdU (Fig. 7D). The results for the limbal cells were qualitatively similar, however, the very small number of cells recovered for the SP hindered a quantitative assessment for this tissue. Overall, these results are consistent with the notion that SP cells and, in fact, the overlapping LSSC cohorts consist mostly of cells that are not rapidly cycling.

To complement these studies, we performed an experiment (Table 2, experiment number 3) conforming to the classical protocol used to identify label-retaining cells (LRCs). BrdU is infused for a prolonged period of time. This causes the labeling of all rapidly dividing cells and of the fraction of the slow-cycling cells that happen to undergo division during the label infusion interval. After a subsequent chase period, only the slow-cycling cells, which remained quiescent or underwent only 1-2 divisions, could retain a detectable concentration of label (Leblond, 1964). Thus, based on the results of the BrdU uptake experiments, we extended the BrdU infusion to the full pump life (14-16 days), to maximize the initial labeling index and chased for a period of 38 days. As expected, after this chase period BrdU$^+$ basal cells were scarce (Fig. 6). In the conjunctival epithelium, prominently stained cells were present in the Goblet cell-rich palpebral and fornical zones (Fig. 6B,C). Fewer BrdU-retaining basal cells were observed in the Goblet cell-free palpebral conjunctiva (Fig. 6B), or in the bulbar area (Fig. 6E). In the limbal epithelium, BrdU label was present in a fraction of the basal cells (Fig. 6E). Cells displaying various levels of staining were observed within the suprabasal strata in both epithelial lineages, in particular near the epithelial surface,

Fig. 6. Immunofluorescence micrographs of BrdU in rabbit ocular surface epithelia. (A,B) Palpebral conjunctiva. The location of the mucocutaneous junction (mcj) is indicated. Arrowheads point to some of the Goblet cells. Frame A shows a representative section from the rabbit subjected to 10 days of BrdU treatment. About 50% of the cells incorporate label (yellow-green fluorescence). Labeling extends to the suprabasal compartment indicating the rapid nature of cell turnover and stratification in this epithelium. Frame B shows an equivalent section from the animal subjected to a 38-day BrdU chase. Label is scant. Within the proliferative basal layer BrdU is present in cells in the Goblet cell-rich zone but it is essentially absent within the basal cells of the highly layered and Goblet-cell free zone proximal to the mucocutaneous junction. (C) Fornical conjunctiva of the same specimen shown in B. In this area the epithelium presents a lobular-like organization and displays substantial BrdU retention in basal cells. (D,E) Sections incorporating bulbar conjunctiva and the limbal (Li) and central corneal (Co) zones. There is substantial BrdU incorporation in all three domains (D). Following the 38-day chase, strong BrdU retention is seen only in the cells of the limbus (E). Bar, 100 μm.
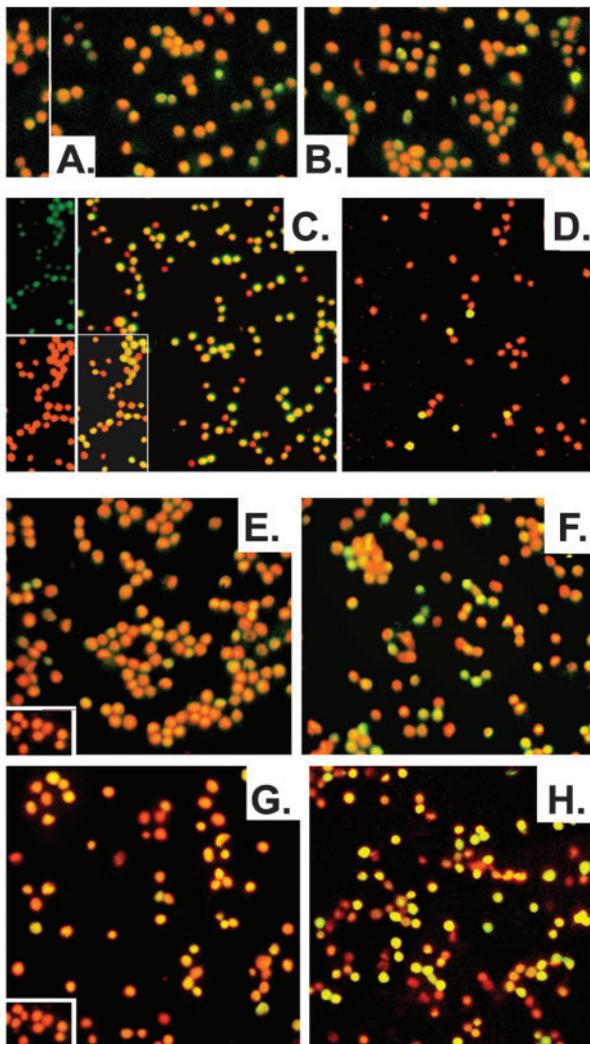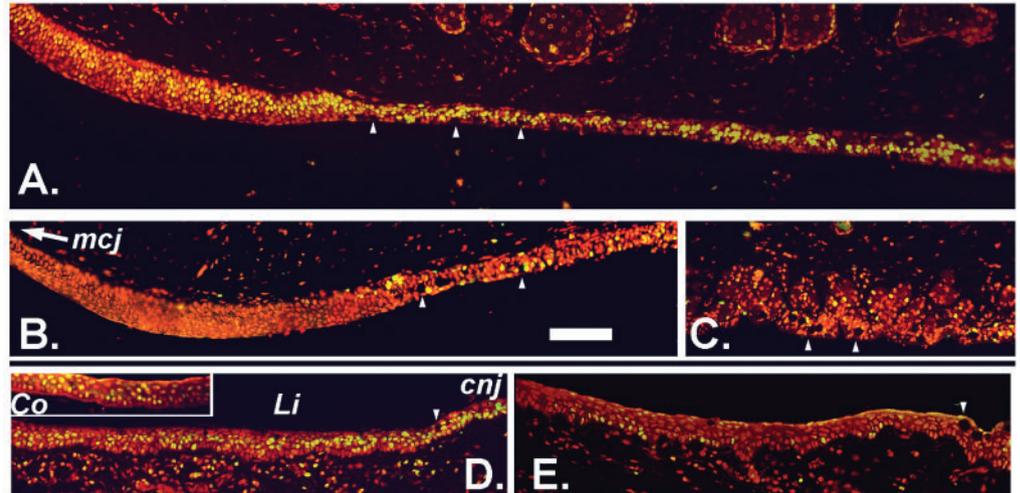
indicating that label disappearance during the 6-week chase interval reflects not its only dilution through multiple cell divisions but also loss through cell exfoliation. Consistent with the tissue immunostaining patterns, cytometer-sorted conjunctival epithelial G0-G1 fraction, which represents the majority of the cell population, contained very few BrdU+ cells (Fig. 7E). In contrast, 22% of the cells in the conjunctival SP sample were BrdU-rich (Fig. 7F; Table 2, experiment number 3). With respect to the study of the limbal cells, we needed to consider that when dealing with a small number of cells (such as in the case of the limbus) the multiple steps involved in Hoechst analysis leads to substantial cell attrition. Thus, given the high degree of overlap between SP and LSSC cohorts and the similarity of BrdU uptake rates observed for both populations (Table 2), we chose to sort limbal cells according to light scattering into LSSC and non-LSSC cohorts, thereby circumventing the Hoechst loading step. Results were similar to those obtained for the SP/non-SP-based conjunctival cell

Fig. 7. Distribution of BrdU in rabbit ocular surface epithelial cells sorted by flow cytometry. (A-D) Representative images of the experiments with limbal and conjunctival cells sorted following a 10-day label infusion. Frames A and B are limbal SP and LSSC cells. Note that in both populations the percentile of BrdU+ cells (yellow-green fluorescence) is low. Images were captured using dual red-green emission filtering. Unlabeled cells are shown as inserts for reference purposes. Frames C and D belong to the adherent cell fractions (Methods) from conjunctival G0-G1 and SP cells, respectively. For this experiment, green and red emissions were captured independently and superimposed, as graphically depicted on the left-hand side of C. Note that in the G0-G1 fraction the majority of cells incorporate BrdU whereas only a few SP cells are BrdU-positive. (E-H) Images from an experiment where the rabbit was infused for the full pump duration (14-16 days) followed by a 38-day label chase. Frames F and E correspond to conjunctival G0-G1 and SP respectively. Frames G and H are from the non-LSSC and LSSC limbal cells. Small inserts are images of BrdU-free nuclei.

Table 2. Percentage of BrdU-positive cells in various flow cytometry fractions obtained from Hoechst-loaded rabbit limbal and conjunctival epithelia

Experiment	Conditions	Tissue	SP	G0/G1	LSSC	non-LSSC
1	10-day infusion	Limbal-cs	13	57	11	51
		Conjunctival-cs	15	47	14	41
2	10-day infusion	Conjunctival-pl	9	87		
3	>14-day infusion	Limbal-cs			18	<1
	38-day chase	Conjunctival-cs	22	<1		

Cs and pl indicate cytospun and plated cells, respectively. All percentiles are based on counting at least 240 cells.

comparison (Fig. 7G,H; Table 2). Only the LSSC population contained a substantial percent of BrdU$^+$ cells.

Further tests of cycling rate were based on the proliferative behavior of the LSSC and SP cells immediately after transference to the in vitro environment. We reasoned that cells that exhibit slow or infrequent cycling in vivo might require a longer time to initiate proliferation in culture than cells that are rapidly cycling. Indeed, rabbit LSSC cells (about half of which are SP cells; Fig. 3), contained a high proportion of the cells that remained quiescent during the first 72 hours after seeding (Fig. 8). In contrast, the great majority of the cells in the much larger general population began to proliferate within the first 48 hours (or, alternatively, may have detached from the plate during this period). Similar results were obtained using conjunctival epithelial cells (data not shown). The cultured CFDA–SE-loaded cells were also sorted according to their Hoechst emission features and analyzed for CFDA fluorescence retention (Table 3). Sixteen hours after seeding, when few cells have completed a round of cell division, the CFDA-SE fluorescence of the average SP cell amounted to about 80% and 70% of that for the G0-G1 or the S-G2/M cells respectively. This initial intensity ratio is consistent with the smaller mass of the SP cell. However, after another 48 hours
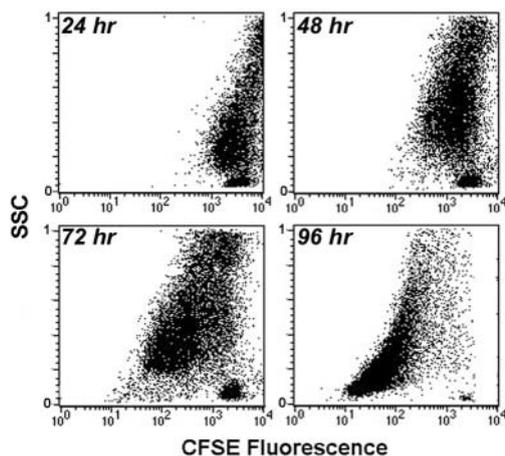
of culture, the fluorescence of the non-SP cells underwent a fourfold reduction, whereas the fluorescence of the SP cells had decreased by only one half. As loss of fluorescence primarily reflects cell division, these studies indicate the slow-cycling nature of the SP cells during the early post-seeding period.

In addition to the studies of cycling rate, we assessed the colony-forming efficiency (CFE) of SP and non-SP cell fractions. Freshly trypsinized limbal and conjunctival rabbit epithelial cells displayed CFEs of between 6-9% after 14 days of culture (based on at least ten experiments in each case). Incubation with Hoechst did not change CFEs. Cell processing through the flow cytometer has only a moderate effect (CFE decreased from 5.3 to 4.2% for the limbal sample; n=2). The CFE for the selected limbal cell G0-G1 fraction, 5.1% (n=3),
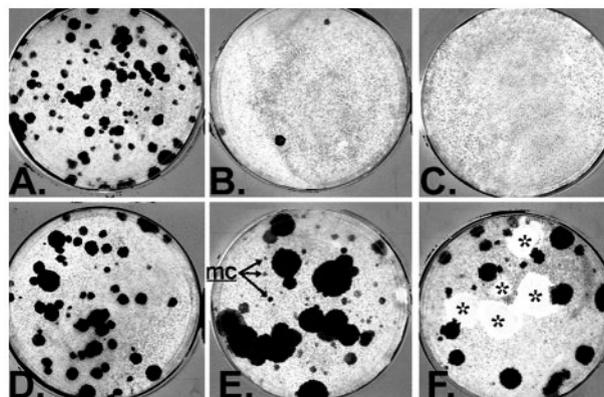

Fig. 9. Clonogenic growth of rabbit limbal G0-G1 and SP cells on 3T3 feeder cells. G0-G1 cell collection was restricted to cells having an FSC range comparable to that of the SP cells. Colonies from G0-G1 (A-C) and SP cells (D-F) were generated from 2000 plated cells after 11 days (A,B) or after 14 days (C,D) of culture. PMA (100 μM) was included in these cultures for 4-72 hours post-plating interval. Note that essentially all colony formation by the G0-G1 cells is arrested whereas a substantial number of colonies grow from the SP cells, and the SP culture contains a substantial number of microcolonies (mc). Microscopic examination showed that most of these colonies consist of small, morphologically undifferentiated cells. (C,F) Fate of microcolonies. Dishes were complemented with 400 limbal epithelial cells and treated with PMA as described for B and E. After 14 days, colonies were present only in the SP dish. These large fast-growing colonies were removed by swiping (clear cell-free areas marked by asterisks on the grayish background generated by the 3T3 cell mat) and the culture was continued for two more weeks. The microcolonies continued to grow to form new large colonies.

Fig. 8. CFDA-SE retention of freshly plated limbal epithelial cells as a function of their SSC. The time elapsed since plating is indicated within each plot. The decrease in CFDA-SE fluorescence primarily reflects cell division. The general population of adherent cells exhibits large decreases in fluorescent intensity in the 24-48, 48-72 and 72-96 hour intervals whereas the great majority of the LSSC cells seem to retain most of the initial fluorescence for the first 72 hours. The experiment shown is representative of two experiments with limbal and two experiments with conjunctival epithelial cells.

Table 3. Yields and CFDA fluorescence in the various cohorts of cultured rabbit limbal cells

Time in culture		SP	G1	S-G2/M	SP/G1 ×100
16 hours	% viable cells	3.4	59.3	12.6	5.7
	CFDA fluorescence*	312	389	463	80
64 hours	% viable cells	0.93	41.9	24.8	2.3
	CFDA fluorescence*	222	110	132	201

*Arbitrary relative units.

was similar to that of the whole population (Fig. 9A). Considering such results, the CFE for rabbit SP cells grown in FCS-hD/F12 was poor, amounting to 2.9±1.2% (n=3) and 3.6±2.0% (n=4), for the limbal (Fig. 9D) and conjunctival epithelia, respectively. Nevertheless, cells within almost all colonies derived from the SP fraction remained small and highly compact for the first 14 days of culture, features associated with undifferentiated cells. In contrast, many of the G0-G1-derived colonies ceased to grow after 8-10 days in culture and developed large irregularly shaped cells indicative of a more differentiated phenotype. To obtain some insight on the proliferative capacity of the SP-derived colonies, three large clones from the rabbit limbal SP culture were serially cultivated using permeable inserts containing a layer of feeder 3T3 cells (Wolosin et al., 2000). We terminated this serial cultivation when a cumulative number of about 10^9 cells were reached. As the three initial colonies represent three founding cells, on average the progeny of each of these cells must have undergone ~35 population doublings, indicating the large proliferative capacity of the founding SP cells.

Finally, we examined the effects of PMA on the SP cells. Addition of PMA to cultured epidermal keratinocytes or corneal epithelial cells induces the majority of cells to cease proliferating and commence differentiation. However, a small subset of cells can selectively withstand this 'differentiative effect' of phorbol esters. Multiple observations suggest that this PMA-resistant cell population consists of stem cells (Hawley-Nelson et al., 1982; Parkinson et al., 1983; Yuspa, 1983; Kruse and Tseng, 1991). Therefore, we tested the effects of PMA on the sorted ocular epithelial cell cohorts. When we added PMA to the G0-G1 population during the 4-72 hours post-plating interval, cells ceased to proliferate and clone production was minimal or nil (Fig. 9B). In contrast, many of the SP cells withstood the effect of PMA and went on to form large colonies (Fig. 9E). Furthermore, during continuous microscopic monitoring of the PMA-treated SP dishes, we noticed the appearance of clusters of four to eight small cells around day 9. By day 14, these same dishes contained multiple visible microcolonies (triple arrow in Fig. 9E). Control experiments where the epithelial cells were seeded at the center of the dish using a plastic ring that was removed on day 3, demonstrated that such microcolonies are unlikely to represent putative satellites originating from cells that have somehow migrated from the original colonies. To explore the long-term behavior of these microcolonies, the large colonies were wiped off (fewer cells were plated in this experiment to reduce the number of PMA-resilient colonies by day 14) and culture was continued for another two weeks. During this time the microcolonies grew to form tightly packed colonies of small cells. The number of these late colonies was far greater than

the number of the PMA-resilient fast growing colonies (Fig. 9F). The PMA-treated G0-G1 dishes failed to generate any such slow-developing colonies (Fig. 9C).

Discussion

Cells displaying an SP phenotype were initially identified in bone marrow as a small cohort of blood progenitors displaying stem cell features (Goodell et al., 1996). We demonstrate in this report that (1) cells with the SP phenotype are present in the conjunctival and limbal/corneal epithelial lineages; (2) within the limbal/corneal epithelium, SP cells are present in the cells from the limbal zone, where the stem cells reside (Schermer et al., 1986; Cotsarelis et al., 1989; Lehrer et al., 1998), but absent from the stem cell-free corneal epithelial domain; (3) at least 50% of the SP cells display a light-scattering phenotype characterized by an extremely low SSC; (4) the ocular surface SP cells display features consistent with adult stem cells; and (5) the LSSC cells display the same stem cell-associated properties as the SP cells. These findings represent a substantial step towards the isolation and characterization of the stem cells present within the ocular anterior surface epithelium.

Our conclusion on the stem cell nature of the isolated ocular surface epithelial SP and LSSC cells are based on a multifaceted examination of the properties of these SP cells. The strongest and most significant evidence is provided by the observation that the SP and LSSC cohorts contain a high proportion of slow-cycling cells, the most recognized feature of stem cells in self-renewing adult tissues. The results of label uptake during the 10-day infusion and label retention after a 14–16-day infusion followed by an extended label chase are consistent. They show that in these populations slightly more than 1% of the cells undergo cell division each day (e.g. in the conjunctival SP, 15% of the cells incorporate label during the 10-day infusion and 22% of the cells incorporated and retained label following the 14–16-day infusion). Thus, we can conclude that in these nearly mature rabbits the average SP and LSSC cell cycles once every 2-3 months.

The manner in which the SP and LSSC cells behaved when placed in culture provided further evidence that these cells are slow-cycling. Relatively quiescent stem cells frequently require a longer time to initiate proliferation upon transference to a cell culture environment when compared with cells that are rapidly dividing (Oostendorp et al., 2000; Ladd et al., 1997; Punzel et al., 2002). These cells remained quiescent for at least the first 72 hours after seeding, whereas the non-SP and non-LSSC cells began to divide within 24-48 hours. Taken together, these results establish the slow-cycling nature of the limbal and conjunctival epithelial SP cells as well as the LSSC cell populations. The extremely low light side-scattering phenotype is indicative of minimal intracellular complexity or 'primitiveness', which is a property consistent with the highly undifferentiated nature of stem cells.

Other major properties ascribed to stem cells from stratified epithelia are their ability to initiate clonal growth and yield colonies consisting of small cells that have a long survival time, known as holoclones (Barrandon and Green, 1987; Wei et al., 1993; Rochat et al., 1994; Pelligrini et al., 1999; Pelligrini et al., 2001; Papini et al., 2003), and the capacity of these cells to survive and clonally proliferate following exposure to PMA

(Hawley-Nelson et al., 1982; Parkinson et al., 1983; Yuspa, 1983; Kruse and Tseng, 1993). Consistent with these features we obtained clones exclusively composed of small cells that displayed a substantial degree of generational capacity and capacity to survive the effect of PMA. These functional features notwithstanding, our SP cells displayed a low (~3%) CFE. A literature search, though, revealed that stem cell-rich fractions exhibiting substantially lower CFEs than the source whole populations have been observed in adult rat epidermis (Pavlovitch et al., 1991) and in neonatal human foreskin (Li et al., 1998). This is remarkable considering that whole populations include a large proportion of suprabasal, differentiated cells. Thus, it is possible that in our CFE assays, the cell progeny present in the non-SP G0-G1 fraction display much better clone forming abilities than the SP cells. Relevant to this hypothesis, hematopoietic stem cells with long-term bone marrow repopulating capacity have been shown to have minimal to no clonal capacity (Sutherland et al., 1990: Haylock et al., 1992). Yet, when cultured under standard conditions the same cells give rise to a progeny of clonogenic cells, presumably as a result of initial differentiation events. Additionally, as suggested others (Li et al., 1998) short-term cultures may be inappropriate for assessing the full proliferative capacity of epithelial fractions enriched in stem cells. In the PMA-exposed SP cell dishes slow-forming colonies were substantially more numerous than the large colonies formed within the first two weeks (see Fig. 9E,F). Thus, CFE calculation based exclusively on fast-forming colonies may not be valid as an assessment tool for stem cell enrichment, at least until optimal conditions for the in vitro activation of these cells are identified (Ladd et al., 1997).

The majority of the SP phenotype in the ocular surface cells is caused by ABCG2 activity, as evidenced by the marked reduction in SP cells by fumitremorgin C. However, the ABCG2 expression patterns seen with immunohistochemistry (Fig. 1) suggest the existence of significantly higher numbers of ABCG2$^+$ cells than SP cells. Multiple factors could account for this apparent discrepancy. The SP is a function of the ratio between the passive influx and active efflux of Hoechst. Thus, part of the SP phenomenon may reflect low Hoechst passive cell membrane permeability, due to a unique lipid composition, relative paucity of 'leak' channels, or a very limited surface membrane. In addition, certain cells displaying an ABCG2$^+$ phenotype by immunohistochemistry may not have enough efflux activity to cancel the passive influx rate. Given the cluster organization of the ABCG2 antigen in limbal epithelial cells (Fig. 2), it is tempting to speculate that the SP cells are restricted to those ABCG2$^+$ cells located at the center of each cluster, in a manner analogous to the hierarchical epidermal proliferative unit (Potten, 1974; Potten, 1991).

In summary, we have found that the SP phenotype is useful for isolating fractions of limbal and conjunctival epithelial basal cells that are enriched in stem cells. Furthermore, our studies indicate that a light-scatter phenotype characterized by extremely low side scattering may constitute an alternative means for the isolation of stem cells from the ocular surface epithelia. The ability of either of these cells to reconstitute epithelia in vivo remains to be evaluated.

References

Abbott, B. L., Colapietro, A. M., Barnes, Y., Marini, F., Andreeff, M. and Sorrentino, B. P. (2002). Low levels of ABCG2 expression in adult AML blast samples. *Blood* **100**, 4594-4601.

Alison, M. R. (2003). Tissue-based stem cells: ABC transporter proteins take centre stage. *J. Pathol.* **200**, 547–550.

Barrandon, Y. and Green, H. (1987). Three clonal types of keratinocyte with different capacities for multiplication. *Proc. Natl. Acad. Sci. USA* **84**, 2302-2306.

Bhattacharya, S., Jackson, J. D., Das, A. V., Thoreson, W. B., Kuszynski, C., James, J., Joshi, S. and Ahmad, I. (2003). Direct Identification and Enrichment of Retinal Stem Cells/Progenitors by Hoechst Dye Efflux Assay. *Invest. Ophthalmol. Vis. Sci.* **44**, 2764-2773.

Bickenbach, J. R. (1981). Identification and behavior of label-retaining cells in oral mucosa and skin. *J. Dent. Res.* **60**, 1611-1620.

Bradfute, S. B. and Goodell, M. A. (2003). Adenoviral transduction of mouse hematopoietic stem cells. *Mol. Ther.* **7**, 334-340.

Braun, K. M., Niemann, C., Jensen, U. B., Sundberg, J. P., Silva-Vargas, V. and Watt, F. M. (2003). Manipulation of stem cell proliferation and lineage commitment: visualisation of label-retaining cells in holemounts of mouse epidermis. *Development* **130**, 5241-5255.

Chen, W., Ishikawa, M., Yamaki, K. and Sakuragi, S. (2003). Wistar rat palpebral conjunctiva contains more slow-cycling stem cells that have larger proliferative capacity: implication for conjunctival epithelial homeostasis. *Jpn. J. Ophthalmol.* **47**, 119-128.

Civin, C. I. (1992). Identification and positive selection of human progenitor/stem cells for bone marrow transplantation. *Prog. Clin. Biol. Res.* **377**, 461-472.

Cotsarelis, G., Cheng, S. Z., Dong, G., Sun, T. T. and Lavker, R. M. (1989). Existence of slow-cycling limbal epithelial basal cells that can be preferentially stimulated to proliferate: implications on epithelial stem cells. *Cell* **57**, 201-209.

Davis, J. A. and Reed, R. R. (1996). Role of Olf-1 and Pax-6 transcription factors in neurodevelopment. *J. Neurosci.* **16**, 5082-5094.

Fortunel, N., Batard, P., Hatzfeld, A., Monier, M. N., Panterne, B., Lebkowski, J. and Hatzfeld, J. (1998). High proliferative potential-quiescent cells: a working model to study primitive quiescent hematopoietic cells. *J. Cell Sci.* **111**, 1867-1875.

Goodell, M. A., Brose, K., Paradis, G., Conner, A. S. and Mulligan, R. C. (1996). Isolation and functional properties of murine hematopoietic stem cells that are replicating in vivo. *J. Exp. Med.* **183**, 1797-1806.

Hawley-Nelson, P., Stanley, J. R., Schmidt, J., Gullino, M. and Yuspa, S. H. (1982). The tumor promoter, 12-O-tetradecanoylphorbol-13-acetate accelerates keratinocyte differentiation and stimulates growth of an unidentified cell type in cultured human epidermis. *Exp. Cell. Res.* **137**, 155-167.

Haylock, D. N., To, L. B., Dowse, T. L., Juttner, C. A. and Simmons, P. J. (1992). Ex vivo expansion and maturation of peripheral blood CD34+ cells into the myeloid lineage. *Blood* **80**, 1405–1412.

Kim, M. and Morshead, C. (2003). Morshead Distinct Populations of Forebrain Neural Stem and Progenitor Cells Can Be Isolated Using Side-Population Analysis. *J. Neurosci.* **23**, 10703-10709.

Koroma, B. M., Yang, J. M. and Sundin, O. H. (1997). The Pax-6 homeobox gene is expressed throughout the corneal and conjunctival epithelia. *Invest. Ophthalmol. Vis. Sci.* **38**, 108-120.

Kruse, F. E., Chen, J. J., Tsai, R. J. and Tseng, S. C. (1990). Conjunctival transdifferentiation is due to the incomplete removal of limbal basal epithelium. *Invest. Ophthalmol. Vis. Sci.* **31**, 1903-1913.

Kruse, F. E. and Tseng, S. C. (1993). A tumor promoter-resistant subpopulation of progenitor cells is larger in limbal epithelium than in corneal epithelium. *Invest. Ophthalmol. Vis. Sci.* **34**, 2501-2511.

Ladd., A. C., Pyatt, R., Gothot, A., Rice, S., McMahel, J., Traycoff, C. M. and Srour, E. F. (1997). Orderly process of sequential cytokine stimulation is required for activation and maximal proliferation of primitive human bone marrow CD34+ hematopoietic progenitor cells residing in G0. *Blood* **90**, 658-668.

Lassalle, B., Bastos, H., Louis, J. P., Riou, L., Testart, J., Dutrillaux, B., Fouchet, P. and Allemand, I. (2003). Side Population cells in adult mouse testis express Bcrp1 gene and are enriched in spermatogonia and germinal stem cells. *Development* **131**, 479-487.

Leblond, C. P. (1964). Classification of cell populations on the basis of their proliferative behavior. *Natl. Cancer Inst. Monogr.* **14**, 119-50.

Lechner, A., Leech, C. A., Abraham, E. J., Nolan, A. L. and Habener, J. F. (2002). Nestin-positive progenitor cells derived from adult human pancreatic islets of Langerhans contain side population (SP) cells defined by expression of the ABCG2 (BCRP1) ATP-binding cassette transporter. *Biochem. Biophys. Res. Commun.* **293**, 670-674.

Lehrer, M. S., Sun, T. T. and Lavker, R. M. (1998). Strategies of epithelial repair: modulation of stem cell and transit amplifying cell proliferation. *J. Cell Sci.* **111**, 2867-2875.

Li, A., Simmons, P. J. and Kaur, P. (1998). Identification and isolation of candidate human keratinocyte stem cells based on cell surface phenotype. *Proc. Natl. Acad. Sci. USA* **31**, 3902-3907.

Nagasaki, T. and Zhao, J. (2005). Uniform distribution of epithelial stem cells in the bulbar conjunctiva. *Invest. Ophthalmol. Vis. Sci.* **46**, 126-132.

Nakanishi, T., Doyle, L. A., Hassel, B., Wei, Y., Bauer, K. S., Wu, S., Pumplin, D. W., Fang, H. B. and Ross, D. D. (2003). Functional characterization of human breast cancer resistance protein (BCRP, ABCG2) expressed in the oocytes of Xenopus laevis. *Mol. Pharmacol.* **641**, 452-462.

Morris, R. J. and Potten, C. S. (1994). Slowly cycling (label-retaining) epidermal cells behave like clonogenic stem cells in vitro. *Cell Prolif.* **27**, 279-289.

Maliepaard, M., Scheffer, G. L., Faneyte, I. F., van Gastelen, M. A., Pijnenborg, A. C., Schinkel, A. H., van de Vijver, M. J., Scheper, R. J. and Schellens, J. H. (2001). Subcellular localization and distribution of the breast cancer resistance protein transporter in normal human tissues. *Cancer Res.* **61**, 3458-3464.

Moyer, P. D., Kaufman, A. H., Zhang, Z., Kao, C. W., Spaulding, A. G. and Kao, W. W. (1996). Conjunctival epithelial cells can resurface denuded cornea, but do not transdifferentiate to express cornea-specific keratin 12 following removal of limbal epithelium in mouse. *Differentiation* **60**, 31-38.

Murayama, A., Matsuzaki, Y., Kawaguchi, A., Shimazaki, T., and Okano, H. (2002). Flow cytometric analysis of neural stem cells in the developing and adult mouse brain. *J. Neurosci. Res.* **69**, 837-847.

Oostendorp, R. A., Audet, J. and Eaves, C. J. (2000). High-resolution tracking of cell division suggests similar cell cycle kinetics of hematopoietic stem cells stimulated in vitro and in vivo. *Blood* **95**, 855-862.

Ozvegy, C., Litman, T., Szakads, G., Nagy, Z. and Bates, S. (2001). Functional Characterization of the Human Multidrug Transporter, ABCG2, Expressed in Insect Cells. *Biochem. Biophys. Res. Commun.* **285**, 111–117.

Papini, S., Cecchetti, D., Campani, D., Fitzgerald, W., Grivel, J. C., Chen, S., Margolis, L. and Revoltella, R. P. (2003). Isolation and clonal analysis of human epidermal keratinocyte stem cells in long-term culture. *Stem Cells* **21**, 481-494.

Parkinson, E. K., Grabham, P. and Emmerson, A. (1983). A subpopulation of cultured human keratinocytes which is resistant to the induction of terminal differentiation-related changes by phorbol, 12-myristate, 13-acetate: evidence for an increase in the resistant population following transformation. *Carcinogenesis* **4**, 857-861.

Pavlovitch, J. H., Rizk-Rabin, M., Jaffray, P., Hoehn, H. and Poot, M. (1991). Characteristics of homogeneously small keratinocytes from newborn rat skin: possible epidermal stem cells. *Am. J. Physiol.* **261**, C964-C972.

Pellegrini, G., Golisano, O., Paterna, P., Lambiase, A., Bonini, S., Rama, P. and de Luca, M. (1999). Location and clonal analysis of stem cells and their differentiated progeny in the human ocular surface. *J. Cell Biol.* **145**, 769-782.

Pellegrini, G., Dellambra, E., Golisano, O., Martinelli, E., Fantozzi, I., Bondanza, S., Ponzin, D., McKeon, F. and de Luca, M. (2001). p63 identifies keratinocyte stem cells. *Proc. Natl. Acad. Sci. USA* **98**, 3156-3161.

Potten, C. S. (1991). Regeneration in epithelial proliferative units as exemplified by small intestinal crypts. *CIBA Found. Symp.* **160**, 54-71.

Potten, C. S. (1974). The epidermal proliferative unit: the possible role of the central basal cell. *Cell Tissue Kinet.* **7**, 77-88.

Punzel, M., Zhang, T., Liu, D., Eckstein. V. and Ho, A. D. (2002). Functional analysis of initial cell divisions defines the subsequent fate of individual human CD34(+)CD38(–) cells. *Exp. Hematol.* **30**, 464-472.

Rabindran, S. K., Ross, D. D., Doyle, L. A., Yang, W. and Greenberger, L. M. (2000). Fumitremorgin C reverses multidrug resistance in cells transfected with the breast cancer resistance protein. *Cancer Res.* **60**, 47-50.

Robey, R. W., Honjo, Y., van de Laar, A., Miyake, K., Regis, J. T., Litman, T. and Bates, S. E. (2001). A functional assay for detection of the mitoxantrone resistance protein, MXR (ABCG2). *Biochim. Biophys. Acta.* **1512**, 171-182.

Rochat, A., Kobayashi, K. and Barrandon, Y. (1994). Location of stem cells of human hair follicles by clonal analysis. *Cell* **76**, 1063-1073.

Scharenberg, C. W., Harkey, M. A. and Torok-Storb, B. (2002). The ABCG2 transporter is an efficient Hoechst 33342 efflux pump and is preferentially expressed by immature human hematopoietic progenitors. *Blood* **99**, 507-512.

Schermer, A., Galvin, S. and Sun, T. T. (1986). Differentiation-related expression of a major 64 K corneal keratin in vivo and in culture suggests limbal location of corneal epithelial stem cells. *J. Cell Biol.* **103**, 49-62.

Silvestri, F., Banavali, S., Baccarani, M. and Preisler, H. D. (1992). The CD34 hemopoietic progenitor cell associated antigen: biology and clinical applications. *Haematologica* **77**, 265-273.

Summer, R., Kotton, D. N., Sun, X., Ma, B., Fitzsimmons, K. and Fine, A. (2003). SP (Side Population) Cells and Bcrp1 Expression in Lung. *Am. J. Physiol. Lung Cell Mol. Physiol.* **285**, L97-L104.

Sutherland, H. J., Lansdorp, P. M., Henkelman, D. H., Eaves, A. C. and Eaves, C. J. (1990). Functional characterization of individual human hematopoietic stem cells cultured at limiting dilution on supportive marrow stromal layers. *Proc. Natl. Acad. Sci. USA* **87**, 3584-3588.

Townsend, W. M. (1991). The limbal palisades of Vogt. *Trans. Am. Ophthalmol. Soc.* **89**, 721-756.

Tumbar, T., Guasch, G., Greco, V., Blanpain, C., Lowry, W. E., Rendl, M. and Fuchs, E. (2004). Defining the epithelial stem cell niche in skin. *Science* **303**, 359-363.

Uchida, N., Dykstra, B., Lyons, K. J., Leung, F. Y. and Eaves, C. J. (2003). Different in vivo repopulating activities of purified hematopoietic stem cells before and after being stimulated to divide in vitro with the same kinetics. *Exp. Hematol.* **31**, 1338-1347.

Watanabe, H., Okano, T., Tano, Y., Watanabe, K., Nishida, K., Yamato, M., Umemoto, T., Sumide, T., Yamamoto, K. and Maeda, N. (2004). Human limbal epithelium contains side population cells expressing the ATP-binding cassette transporter ABCG2. *FEBS Lett.* **565**, 6-10.

Wei, Z. G., Wu, R. L., Lavker, R. M. and Sun, T. T. (1993). In vitro growth and differentiation of rabbit bulbar, fornix, and palpebral conjunctival epithelia. Implications on conjunctival epithelial transdifferentiation and stem cells. *Invest Ophthalmol. Vis. Sci.* **34**, 1814-1828.

Wei, Z. G., Cotsarelis, G., Sun, T. T. and Lavker, R. M. (1995). Label-retaining cells are preferentially located in fornical epithelium: implications on conjunctival epithelial homeostasis. *Invest. Ophthalmol. Vis. Sci.* **36**, 236-246.

Wei, Z. G., Sun, T. T. and Lavker, R. M. (1996). Rabbit conjunctival and corneal epithelial cells belong to two separate lineages. *Invest. Ophthalmol. Vis. Sci.* **37**, 523-533.

Wirtschafter, J. D., Ketcham, J. M., Weinstock, R. J., Tabesh, T. and McLoon, L. K. (1999). Mucocutaneous junction as the major source of replacement palpebral conjunctival epithelial cells. *Invest. Ophthalmol. Vis. Sci.* **40**, 3138-3146.

Wolosin, J. M, Xiong, X., Schutte, M., Stegman, Z. and Tieng, A. (2000). Stem cells and differentiation stages in the limbo-corneal epithelium. *Prog. Retin. Eye Res.* **19**, 223-255.

Wolosin, J. M., Schutte, M., Zieske, J. D. and Budak, M. T. (2002). Changes in connexin43 in early ocular surface development. *Curr. Eye Res.* **24**, 430-438.

Wolosin, J. M., Budak, M. T. and Akinci, M. A. M. (2004). Ocular surface epithelial and stem cell development. *Intl. J. Dev. Biol.* **48**, 981-991.

Yuspa, S. H. (1983). Alterations in epidermal functions resulting from exposure to initiators and promoters of carcinogenesis. *Curr. Probl. Dermatol.* **11**, 227-241.

Zhou, S., Schuetz, J. D., Bunting, K. D., Colapietro, A. M., Sampath, J., Morris, J. J., Lagutina, I., Grosveld, G. C., Osawa, M., Nakauchi, H. and Sorrentino, B. P. (2001). The ABC transporter Bcrp1/ABCG2 is expressed in a wide variety of stem cells and is a molecular determinant of the side-population phenotype. *Nat. Med.* **7**, 1028-1034.